



DOI: 10.12086/oe.2020.200135

大口径强激光光学元件超精密制造技术研究进展

樊非, 徐曦, 许乔*, 王健, 钟波, 谢瑞清, 雷向阳, 陈贤华, 汪圣飞, 侯晶, 邓文辉, 安晨辉, 周炼, 赵世杰, 廖德锋, 朱玉洁

中国工程物理研究院激光聚变研究中心, 四川 绵阳 621900

摘要: 惯性约束聚变高功率固体激光装置研制对大口径光学元件提出了全频段精度控制指标要求, 以及高效率、批量化制造需求。本文围绕“超精密、确定性”强激光光学元件全流程制造方法, 总结了近几年大口径强激光光学元件超精密制造技术取得的重要进展, 重点介绍了单点金刚石超精密切削技术、非球面超精密数控磨削技术、确定性抛光技术等一系列关键技术, 以及相关工艺及装备在强激光光学元件批量制造流程线中的应用情况。

关键词: 高功率固体激光装置; 大口径光学元件; 光学超精密制造技术; 确定性抛光

中图分类号: TH74

文献标志码: A

引用格式: 樊非, 徐曦, 许乔, 等. 大口径强激光光学元件超精密制造技术研究进展[J]. 光电工程, 2020, 47(8): 200135

Progress on ultra precision manufacturing technology of large-aperture high-power laser optics

Fan Fei, Xu Xi, Xu Qiao*, Wang Jian, Zhong Bo, Xie Ruiqing, Lei Xiangyang, Chen Xianhua, Wang Shengfei, Hou Jing, Deng Wenhui, An Chenhui, Zhou Lian, Zhao Shijie, Liao Defeng, Zhu Yujie

Research Centre of Laser Fusion, China Academy of Engineering Physics, Mianyang, Sichuan 621900, China

Abstract: The construction of high-power solid-state laser facility for inertial confinement fusion requires to precisely control the full-spatial frequency error, and realize efficient mass-manufacturing of large-aperture optics. This review summarizes the recent critical progress in manufacturing of large-aperture optics in high-power laser facility. It also emphasizes the technologies such as single point diamond fly-cutting, and aspheric ultra-precision grinding, as well as deterministic polishing, based on the deterministic ultra-precision process manufacturing method. In addition, the application status of these key technologies in the mass-manufacturing chain was stated specifically.

Keywords: high-power laser facility; large-aperture optics; optical ultra-precision manufacturing technology; deterministic polishing

Citation: Fan F, Xu X, Xu Q, *et al.* Progress on ultra precision manufacturing technology of large-aperture high-power laser optics[J]. *Opto-Electronic Engineering*, 2020, 47(8): 200135

收稿日期: 2020-04-21; 收到修改稿日期: 2020-06-20

作者简介: 国家科技重大专项(2017ZX04022001-101)

作者简介: 樊非(1987-), 男, 硕士, 助理研究员, 主要从事光学超精密加工的研究。E-mail: fanfei65790299@163.com

通信作者: 许乔(1972-), 男, 博士, 研究员, 主要从事先进光学制造的研究。E-mail: xuqiao@vip.sina.com

版权所有©2020 中国科学院光电技术研究所

1 引言

用于惯性约束聚变(inertial confinement fusion, ICF)研究的高功率固体激光装置是当今规模最大、结构最复杂且系统性极强的光学系统工程,需要上万件大口径强激光光学元件,包括磷酸盐钽玻璃放大片和平面反射镜、非球面聚焦透镜、衍射元件,以及大口径非线性激光晶体等^[1]。为保证激光装置获得理想的激光光束质量,并实现高通量条件下稳定运行,该类光学元件要求实现极为严苛的全频段精度控制指标,以及满足极致的低缺陷控制要求。同时高功率固体激光装置研制的成组化、模块化和紧凑化研制目标,对大口径强激光光学元件提出了高效率、批量化、工程化的制造要求。

美国劳伦斯·利弗莫尔国家实验室(Lawrence Livermore National Laboratory, LLNL)围绕美国国家点火装置(National Ignition Facility, NIF)的建设,提出了基于功率谱密度(power spectral density, PSD)的光学表面评价方法与技术指标要求,如大口径非球面元件低频误差 $PV \leq \lambda/3 (\lambda=632.8 \text{ nm})$,中频误差 $PSD1 \leq 1.8 \text{ nm}$ 、 $PSD2 \leq 1.1 \text{ nm}$,高频误差 $Rq \leq 1.0 \text{ nm/cm}^2$ ^[1]。在“超精密化”、“数字化”先进光学制造装备及工艺研发计划的支持下,美国联合国际优势工业力量,先后发展了单点金刚石飞切、小工具数控抛光、确定性连续抛光、磁流变抛光等技术,开发了成套装备,将大口径强激光光学元件制造能力提升了十倍以上,满足 NIF 装置建设需要。

围绕我国高功率固体激光装置研制,本研究团队提出了以“超精密、确定性”为核心的强激光光学元

件全流程制造方法,针对激光晶体材料元件的制造需求,突破了单点金刚石超精密切削技术,针对熔石英材料元件的制造需求,突破了非球面超精密数控磨削与确定性抛光等关键技术^[2]。同时,在国家“高档数控机床与基础制造装备”重大专项(04 专项)的支持下,以工艺为牵引,完成 17 台(套)光学超精密制造装备国产化研制,并进行了工艺的集成验证。本文主要针对大口径强激光光学元件超精密制造技术与装备的发展进行综述回顾。

2 单点金刚石超精密切削技术与装备

KDP(Potassium dihydrogen phosphate, 磷酸二氢钾)晶体是目前唯一适用于高功率激光装置的大口径非线性光学晶体,主要用作光学频率转换元件及电光开关器件^[3]。该材料为各向异性软脆晶体,具有易潮解、对温度变化敏感、易开裂等不利于加工的物化性能,使用研磨抛光方法加工极易嵌入抛光粉颗粒,在强激光应用中将导致严重的激光诱导损伤。目前单点金刚石超精密飞切是 KDP 晶体最理想的加工方法^[4-5]。

KDP 晶体飞切加工产生的小尺度波纹误差,给晶体的透射波前添加了周期性扰动,成为强激光非线性增长的噪声源,在高功率情况下容易形成自聚焦丝状破坏^[6]。研究发现,刀具-工件系统不同频率的周期性相对运动误差会复印到加工表面形成波纹误差^[7],因此,这对机床的动态性能提出了极高要求。本研究团队建立了 KDP 晶体超精密飞切机床动态特性的测量与评价平台(如图 1 所示),实现对机床微弱信号(mN

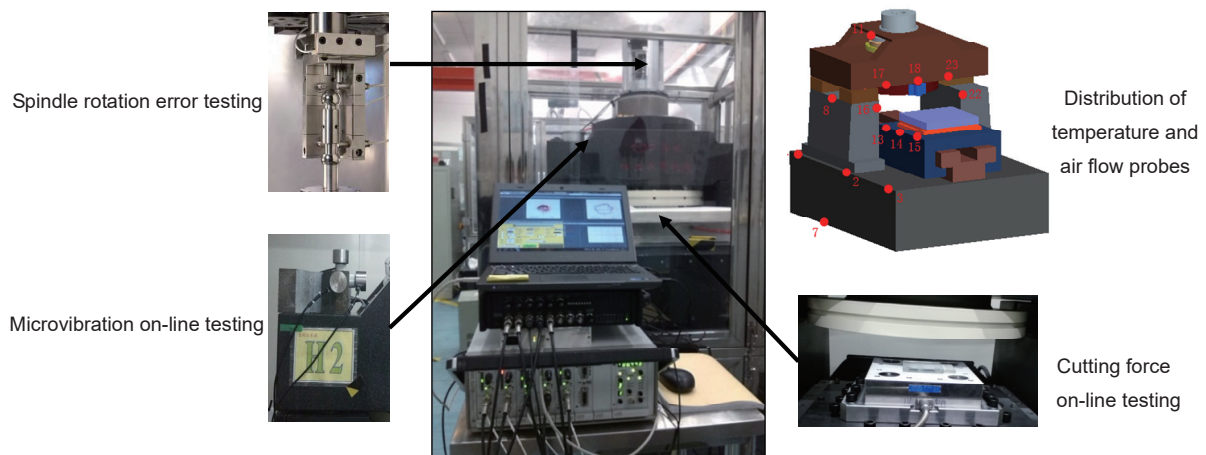


图 1 KDP 晶体超精密飞切机床动态特性的测量与评价平台

Fig. 1 Detection and evaluation platform for dynamic characteristics of KDP crystal single point diamond fly-cutting machine tool

级切削力、mG 级加速度、以及 nm 级位移)的在线动态测量以及特征信息提取^[8]。综合理论分析及实验结果,发现了主轴异步误差、部件自由振动响应特性及组件连接刚度等关键因素对加工表面波纹误差的影响规律,提出了基于频域误差分配的超精密飞切机床设计方法,实现了机床关键部件在中频误差敏感频段响应的有效抑制^[9]。通过以上措施,结合加工系统温度波动、进给波动、刀具微观质量变化等工艺控制方法,加工 400 mm×400 mm×9 mm KDP 晶体典型样件,可获得中频波纹误差 PSD₂≤0.68 nm、透射波前 GMRS≤9.0 nm/cm 的高精度表面,如图 2(a)、2(b)所示。

围绕 KDP 晶体超光滑表面创成,本研究团队从

KDP 晶体基本力学性能出发,结合各向异性弹性、静水压相关塑性模型及方向相关拉应力失效准则,建立了 KDP 晶体的本构模型。通过对切削过程进行模拟仿真,获得了脆-塑转变深度随切削方向的变化,如图 3 所示,给出了最优的切削方向(如(001)晶面内的 45°方向)及对应的脆-塑转变深度(约 150 nm)。在此基础上,提出了脆-塑混合切削模式下的光滑表面形成条件,即在满足脆性切削区的裂纹不扩展到最终加工表面的前提下,选取尽可能大的进给量,以最大效率地获得光滑的塑性表面^[10-11]。基于上述研究结果,对现有 KDP 晶体飞切加工工艺参数进行了优化,可稳定获得了表面粗糙度优于 1 nm 的超光滑表面。

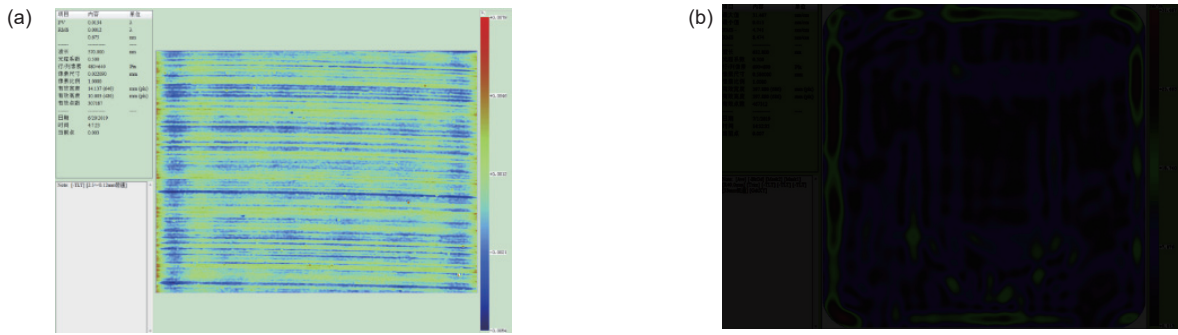


图 2 400 mm×400 mm KDP 晶体超精密加工结果。(a) 中频波纹误差; (b) 透过波前梯度

Fig. 2 Results of 400 mm×400 mm KDP crystal after single point diamond fly-cutting. (a) Result of mid-spatial frequency error; (b) Result of wavefront gradient

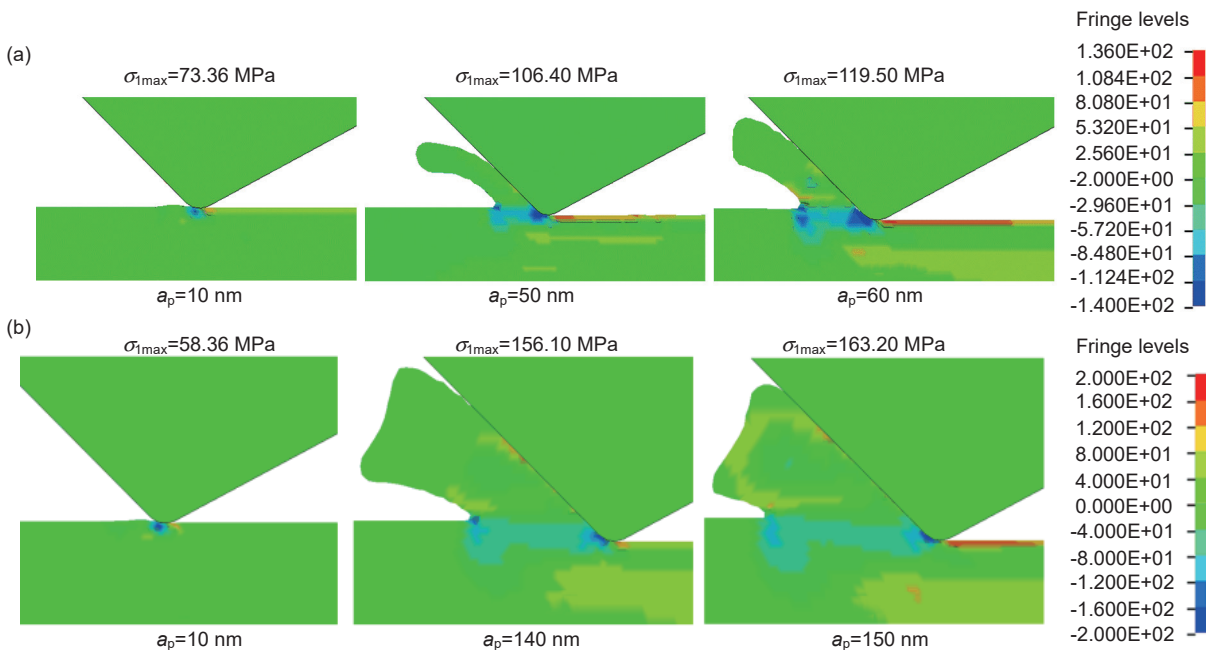


图 3 KDP 晶体脆-塑转变深度仿真结果。(a) 0°方向仿真结果; (b) 45°方向仿真结果

Fig. 3 Simulation results of brittle ductile transition depth in cutting KDP crystal. (a) Simulation results at 0°; (b) Simulation results at 45°

3 非球面超精密数控磨削技术与装备

大功率激光装置所需非球面聚焦透镜通常为高次曲面、类自由曲面，且呈非旋转对称性设计，在系统中起到精密成像、谐波分离、精确聚焦等功能^[2]。本研究团队提出采用超精密平行磨削技术(如图 4 所示)，即基于“XYZ 三正交直线轴+卧式主轴”的超精密数

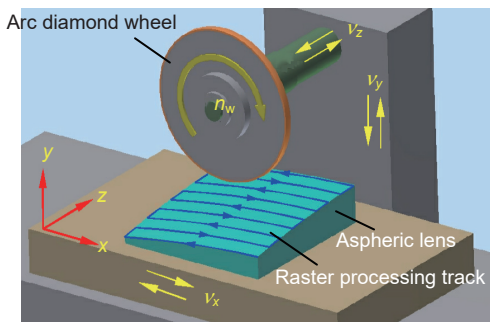


图 4 非球面平行磨削加工原理
Fig. 4 Principle of parallel grinding of aspheric surface

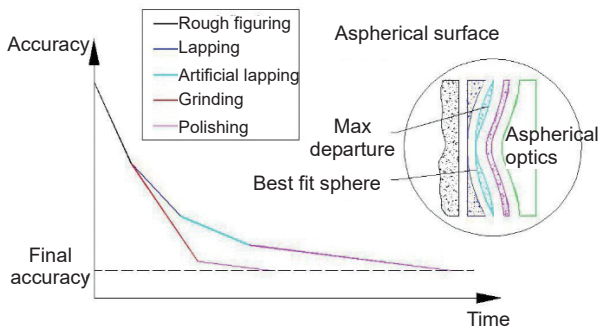
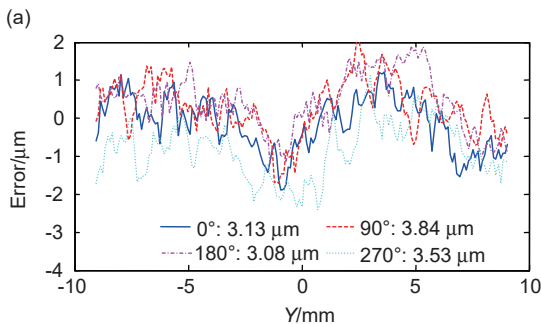


图 5 非球面超精密制造与传统加工技术比较
Fig. 5 Comparison of aspheric ultra-precision manufacturing and traditional processing technology



控磨削机床，通过元件轮廓与砂轮控制点三维坐标精确计算，以光栅包络方式磨削加工，实现异形非旋转对称非球面的快速精密成形^[12]。

采用超精密数控磨削技术实现非球面元件的成形加工，尤其是异形非旋转对称非球面，具有材料去除速率快、面形精度高、便于实现自动化批量制造等优点^[13-14]，如图 5 所示。加工过程中，元件表面点坐标和砂轮运动控制点坐标具有精确的传递函数关系，非球面的成形精度主要取决于砂轮的圆弧轮廓精度和机床的运动控制精度^[15]。

对金刚石砂轮进行精密修整，使圆弧砂轮获得较高的形状精度与锐利度，对元件的加工精度与亚表面缺陷控制尤为重要。本研究团队采用对滚研磨的方式对圆弧砂轮进行在位/离线修整^[16]，如图 6 所示，回转轴正交的金金刚石砂轮和修整砂轮在自转过程中，通过 X/Y/Z 三轴联动控制，金刚石砂轮沿修整砂轮外圆表面在 YZ 平面内作圆弧包络插补，同时修整砂轮沿其轴向作来回进给运动，以实现金刚石砂轮的修形与修锐。采用对滚研磨修整后，金刚石砂轮圆弧轮廓误差小于 $4\ \mu\text{m}$ ，圆度误差小于 $1.5\ \mu\text{m}$ ，如图 7 所示。

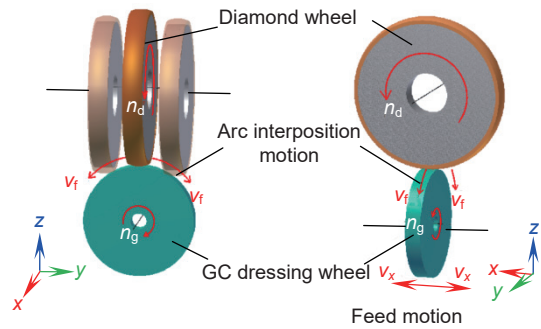


图 6 圆弧金刚石砂轮对滚研磨修整
Fig. 6 The dressing principle of arc diamond wheel by roll abrading

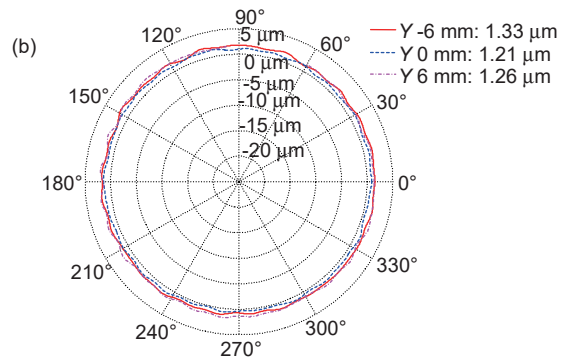


图 7 对滚研磨修整后金刚石砂轮的形状误差和微观形貌。(a) 圆弧轮廓误差; (b) 圆度误差
Fig. 7 Form errors of diamond wheel after dressing. (a) Arc contour error; (b) Roundness error

本研究团队联合厦门大学自主研发了大口径非球面光学元件超精密数控磨削机床, 该机床定位精度优于 $2\ \mu\text{m}$, 重复定位精度优于 $1\ \mu\text{m}$ 。采用该设备与上述工艺方法, 结合磨削液洁净循环处理、砂轮表面完整性控制、砂轮边缘位置加工应力集中抑制^[17-18]、砂轮磨损在线监测控制^[19]等技术, 开展 $500\ \text{mm}\times 500\ \text{mm}$ 口径离轴非球面元件的磨削加工, 面形误差 PV 值达到 $3.3\ \mu\text{m}$, 亚表面缺陷深度在 $5\ \mu\text{m}$ 以内, 如图 8 所示。

4 超精密确定性抛光技术与装备

4.1 气囊高效抛光技术与装备

在保持初始磨削成形精度的基础上, 如何高效去除磨削加工残余表面/亚表面缺陷层, 并使元件达到纳米级表面粗糙度, 是非球面批量制造效能提升的关键问题之一。目前, 气囊抛光是非球面保形抛光的重要手段之一, 对非球面磨削残余亚表面缺陷层快速去除以及低频误差高效收敛具有重要意义。

气囊抛光技术是 20 世纪 90 年代伦敦光学实验室提出的一种新的抛光方法, 并与 Zeeko 公司合作开发了 IRP 系列抛光机床。气囊抛光采用半柔性气囊作抛

光工具, 可保证抛光工具与被抛光曲面工件表面良好吻合, 且通过调节气囊充气压力及主轴转速实现抛光效率和表面质量的提升^[20]。目前, 本研究团队开展的气囊高效抛光技术研究工作主要集中在以下几个方面:

1) 非球面气囊抛光进动控制。运动控制技术是实现非球面加工的基础, 通过气囊进动加工运动学建模, 基于空间旋转矩阵计算非球面任意加工点处气囊抛光机构旋转轴的转角, 实现了气囊位姿的精确控制。在此基础上, 提出了非球面加工气囊位姿优化和多步进动控制算法, 获得了近高斯型叠加去除特性和更为优异的表面纹理。图 9 为楔形非球面气囊抛光实物与原理图。

2) 气囊抛光动态去除函数与面形误差预测。基于摩擦因子、工件曲率、进给速度构建了气囊抛光动态去除函数模型, 提升了非球面加工动态去除函数预测准确性^[21-23]。为准确反映气囊抛光动态过程, 本研究团队创新地提出基于动态去除函数的驻留时间求解算法, 面形仿真过程中采用动态的多去除函数与面形误差反卷积获得动态驻留时间以及相应速度分布, 获得

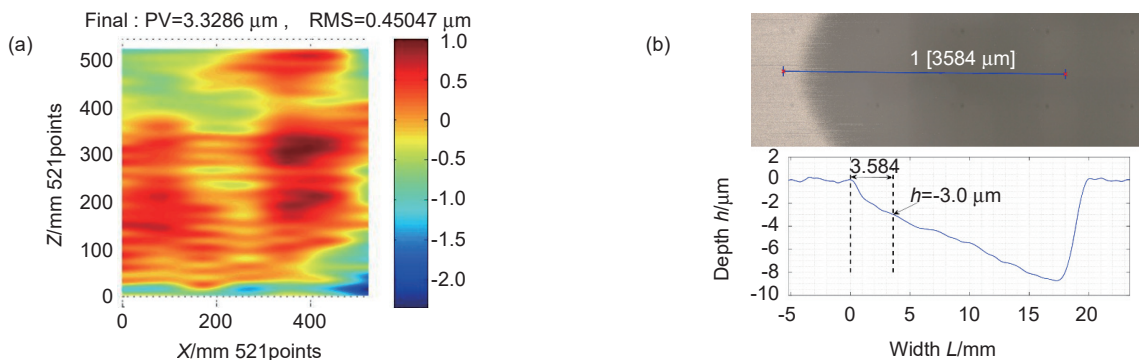


图 8 离轴非球面元件磨削面形误差、亚表面缺陷深度结果。(a) 面形误差结果; (b) 亚表面缺陷深度结果
Fig. 8 Results of off-axis aspheric optics after grinding. (a) Result of form error; (b) Result of sub-surface crack depth

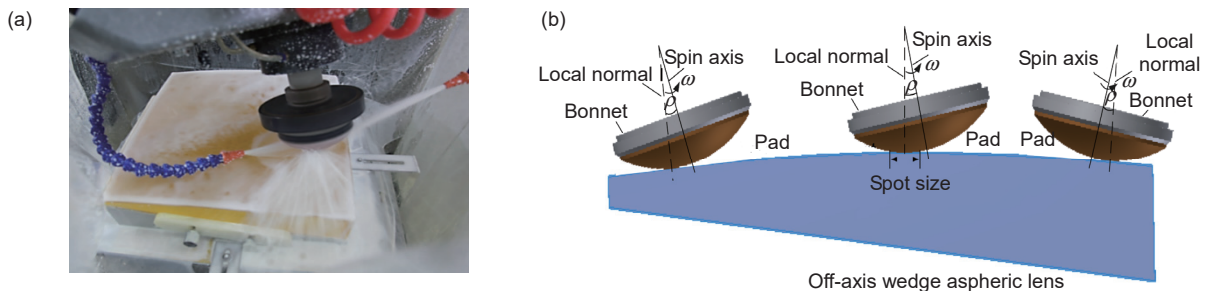


图 9 楔形非球面镜气囊抛光实物图与原理图。(a) 气囊抛光实物图; (b) 气囊抛光原理图

Fig. 9 Bonnet polishing picture and principle for off-axis wedge aspheric lens.
(a) Bonnet polishing picture; (b) Bonnet dressing principle

了更为准确的面形预测结果^[24](如图 10 所示)。

3) 气囊表面磨损与修整处理。通过研究磨损带来的气囊表面特征、抛光力、摩擦系数、去除形态、去除率等物理量的变化规律,建立了“磨损/修整-工具表面形貌-抛光力-去除特性”的传递关系^[25-26],通过“磨损-修整”协调匹配提升了工艺稳定性。图 11 为气囊修整实物与数学模型。

基于以上研究成果,我们将气囊抛光技术应用于离轴楔形非球面聚焦透镜批量制造流程线中^[27],联合国产化 7 轴 5 联动数控气囊抛光机床,保形抛光效率较前期工艺提高约 3 倍^[28]。另外,大口径离轴楔形镜高效修形验证实验结果表明,400 mm 口径非球面平均经 5 次气囊修抛,面形精度可由初始的 5λ 快速收敛 0.33λ,进一步修抛可以达到 0.1λ,梯度可达到 3.4 nm/cm,如图 12 所示。

4.2 确定性全口径抛光技术与装备

采用全口径抛光方法制造大口径光学元件,是降低元件制造成本、缩短加工周期的一条重要技术途径。现阶段,全口径抛光的技术核心是在对大口径光学元件表面材料进行高效抛光去除的同时,进一步提高面形传递的可控性,从而实现全口径抛光面形精度的高效单向收敛^[29-30,32,38]。

本研究团队围绕全口径抛光过程中的工件表面材料去除及精度创成机理、工艺参数确定性控制、表面波纹度及抛光亚表面缺陷抑制等方面开展了深入研究,提出了“确定性全口径抛光”的技术概念^[31-39]。如图 13 所示,该技术采用确定性抛光盘测量与修整技术,严格控制除工件及抛光盘面形误差以外的其它所有非均匀材料去除工艺影响因素,基于复印机制实现抛光盘-工件高精度面形精度传递,结合化学机械抛

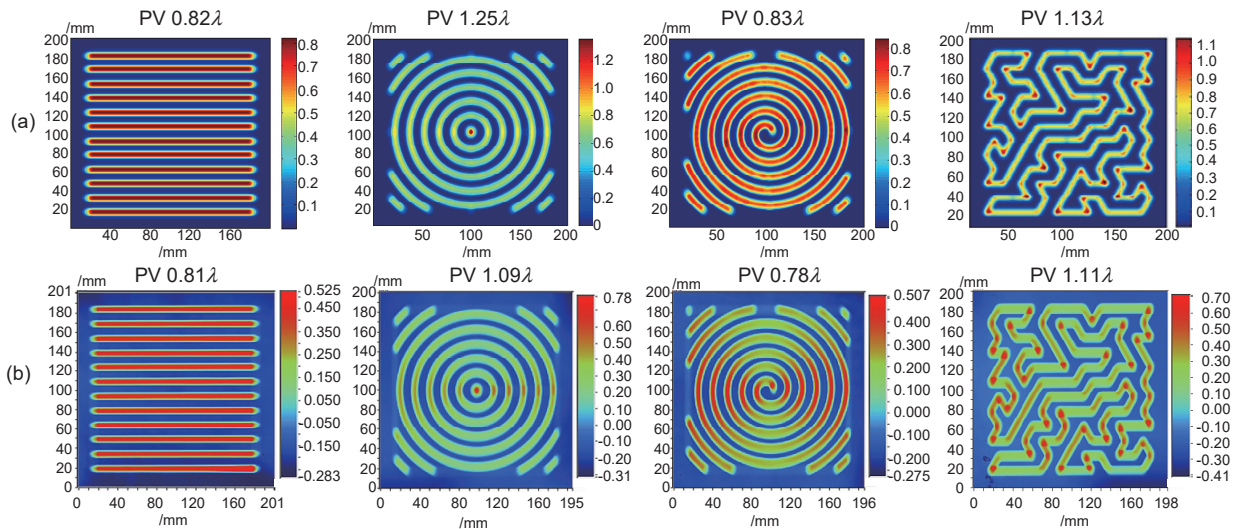


图 10 面形预测与实验验证。(a) 光栅、同心圆、螺旋线、随机四种路径模拟加工结果;

(b) 光栅、同心圆、螺旋线、随机四种路径实际加工结果

Fig. 10 Surface shape prediction and experimental verification. (a) Simulation results of four paths (i.e. raster path, circle path, spiral path and random path); (b) Experimental results of four paths (i.e. raster path, circle path, spiral path and random path)

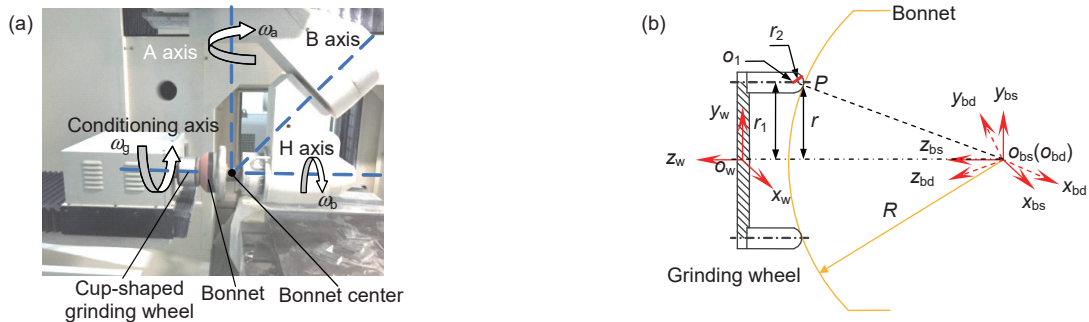


图 11 气囊修整实物与数学模型。(a) 气囊修整实物; (b) 气囊修整数学模型

Fig. 11 Bonnet dressing picture and mathematical model. (a) Bonnet dressing picture; (b) Bonnet dressing mathematical model

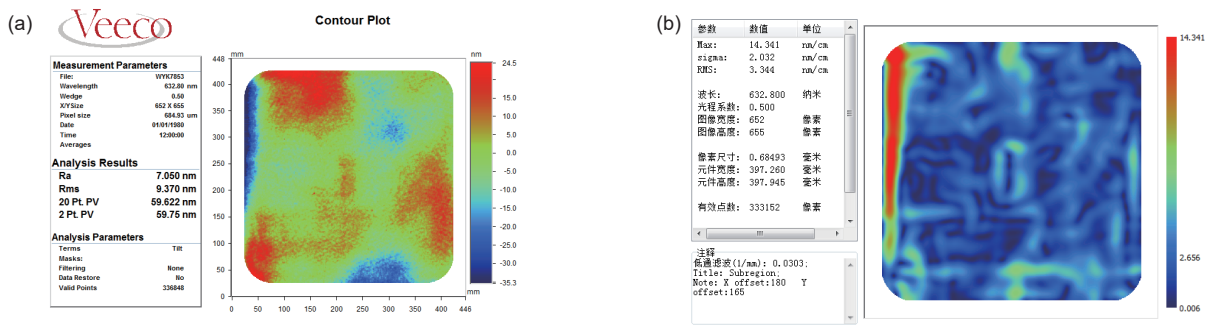


图 12 离轴楔形非球面透镜气囊抛光结果。(a) 透过波前误差; (b) 透过波前梯度

Fig. 12 Results of off-axis wedge aspheric lens by bonnet polishing.

(a) Result of wavefront error; (b) Result of wavefront gradient

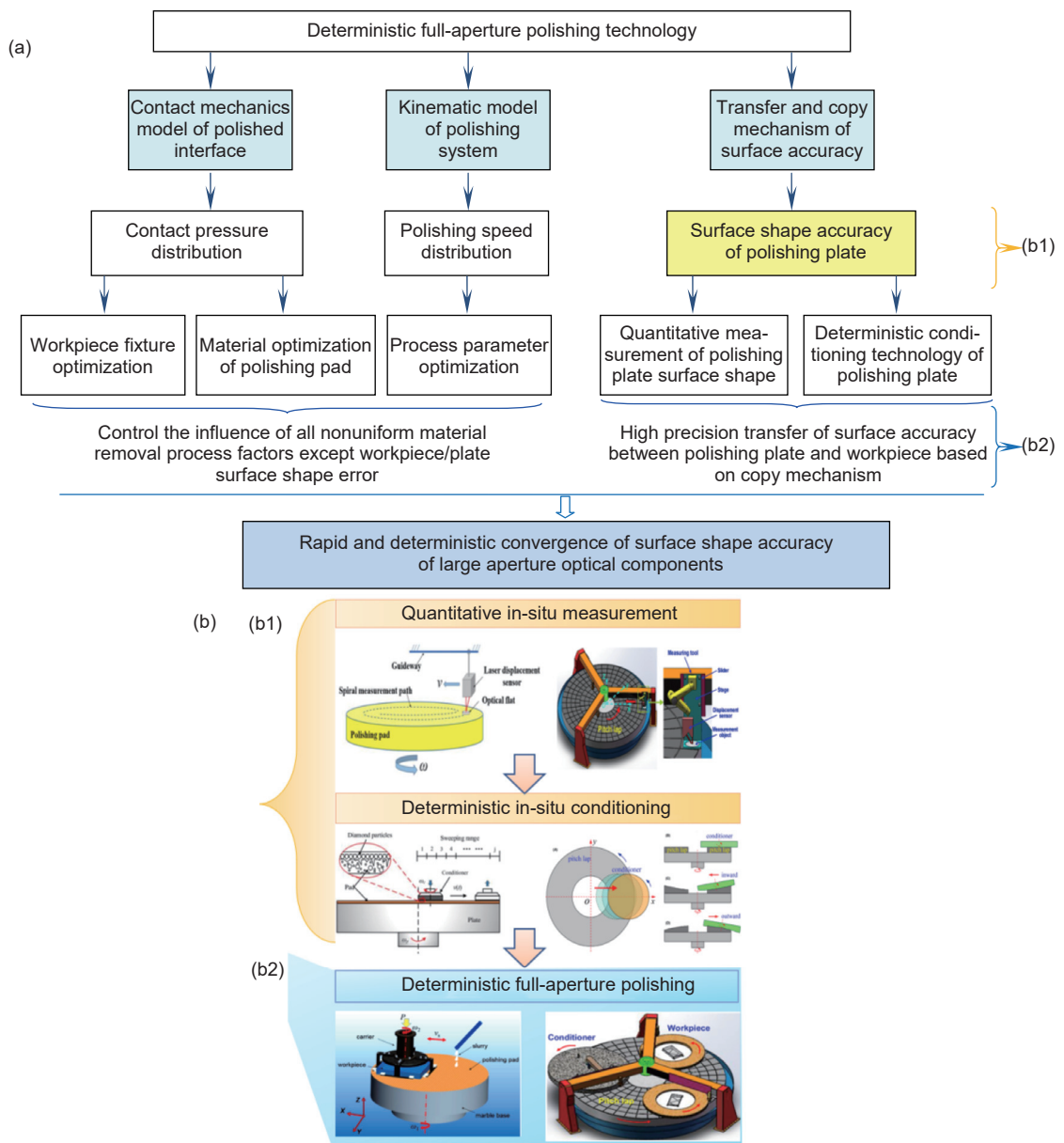


图 13 确定性全口径抛光中元件面形精度控制方法

Fig. 13 Control principle of workpiece precision in deterministic full-aperture polishing

光去除机理, 最终实现大口径光学元件高精度的快速收敛抛光。围绕上述目标的实现, 我们重点解决了光学材料化学机械抛光微观材料去除机理、抛光材料非均匀性去除规律及影响因素识别、精密抛光元件材料去除效率优化、低频/中频表面精度确定性控制、全口径抛光元件表面缺陷控制等关键技术问题^[31,34,37-39]。

围绕不同材料光学元件加工需求, 我们联合国内相关企业自主研发了系列确定性全口径抛光机床(如图 14 所示), 例如采用合成盘的确定性研抛机床, 用于大尺寸激光晶体加工; 采用大尺寸聚氨酯抛光盘的确定性平面快速抛光机床, 用于大口径熔石英基板的加工; 采用大尺寸沥青抛光盘的确定性连续抛光机床, 用于大口径 K9 玻璃反射镜的加工。图 15 为采用上述三类确定性全口径抛光机床的典型加工结果, YAG 晶体、熔石英基板、K9 玻璃反射镜的面形精度 PV 值分别达到 0.08λ , 0.25λ , 0.16λ 。结果表明, 采用新的确定性全口径抛光技术, 可以在显著减少工艺参数调整及检测次数的情况下, 提高元件的抛光精度, 从而使得元件的生产效率得到大幅提升。

4.3 低制度小工具数控抛光技术

沥青小工具抛光技术是最早发展的计算机控制光学表面成形技术(computer controlled optical surfacing, CCOS)。目前, 沥青小工具抛光技术在大口径强激光非球面光学元件制造流程线中主要承担元件全频段误差收敛达标, 提高表面质量的功能。围绕低频误差高精度确定性修正、中高频误差匀滑修正的工艺需求, 我们主要开展了以下两个方面的工作:

1) 针对低频误差高精度确定性修正, 主要从实现去除函数稳定性控制方面开展研究。前期研究发现采用传统沥青小工具开展非球面加工时去除函数存在空间畸变, 该畸变主要由工具局部非球面度和工具刚度共同造成^[40-42]。通过优化沥青抛光工具结构, 提升工具柔性, 在非球面元件表面不同位置获得了幅值和形态基本一致的去除函数。建立了基于故障模式影响及危害度分析方法(failure mode, effects and criticality analysis, FMECA)的去除函数稳定性影响因素分析模型, 探析了抛光盘形貌、抛光盘硬度、抛光液浓度等因素对去除函数的影响规律。如图 16 所示, 去除速率



图 14 采用不同抛光盘类型的确定性全口径抛光机床。

(a) 确定性平面研磨机; (b) 确定性快速抛光机床; (c) 确定性连续抛光机床

Fig. 14 The deterministic full-aperture polishers with different kinds of plate materials.
(a) Deterministic plane lap-polisher; (b) Deterministic rapid polisher; (c) Deterministic continuous polisher

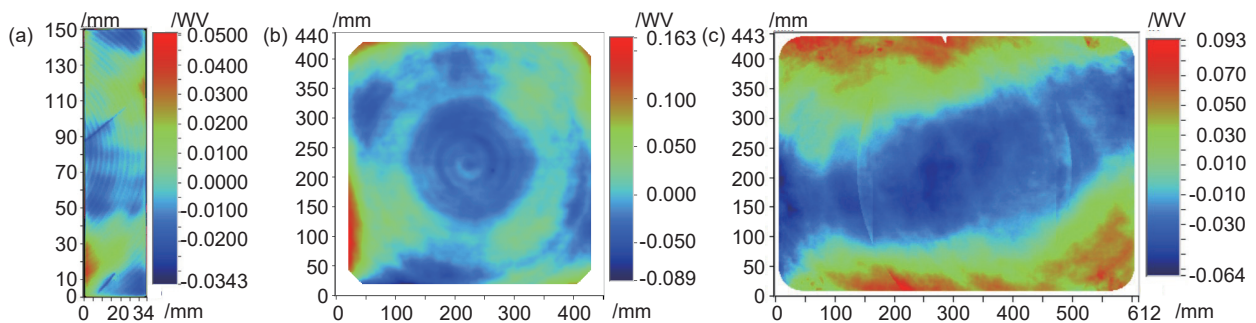


图 15 确定性全口径抛光加工典型实验结果。

(a) YAG 晶体(PV $\leq 0.08\lambda$); (b) 熔石英基板(PV $\leq 0.25\lambda$); (c) K9 玻璃(PV $\leq 0.16\lambda$)

Fig. 15 The typical processing results of the deterministic full-aperture polishers.
(a) YAG crystal (PV $\leq 0.08\lambda$); (b) Fused silica (PV $\leq 0.25\lambda$); (c) K9 glass (PV $\leq 0.16\lambda$)

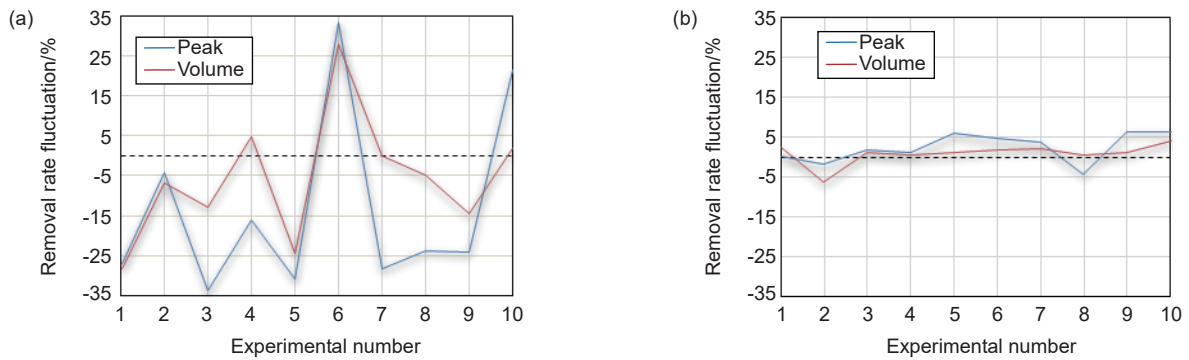


图 16 去除速率稳定性控制实验统计。(a) 未有效控制; (b) 基于 FMECA 控制

Fig. 16 Experimental statistics of removal rate stability control. (a) No effective control; (b) Based on FMECA control

波动由大于 $\pm 30\%$ 降至小于 $\pm 7\%$, 提升了小工具数控抛光过程的不确定性, 为实现低频误差快速收敛奠定了重要基础。

2) 针对中高频误差匀滑修正, 建立了基于弹性理论的小工具数控抛光中高频误差参数化匀滑修正模型。仿真及实验验证结果表明, 中频误差收敛速度与抛光模材料、压力、转速、空间周期均相关, 光学元件表面波纹误差随抛光时间增长呈指数型收敛。如图

17 所示, 所建立的匀滑模型与实际收敛误差小于 5%, 可有效指导大口径光学元件中高频误差的平滑修正加工, 实现了 PSD 的快速收敛。

通过以上研究成果的应用, 实现了 400 mm \times 400 mm 非球面楔形聚焦透镜高效加工, 透过波前误差 PV $\leq 0.1\lambda$ 、中频误差 PSD1 ≤ 1.76 nm, 满足设计指标要求(如图 18 所示)。

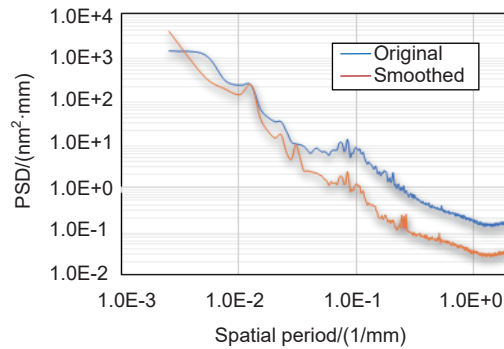


图 17 参数化匀滑修正中高频误差实验结果

Fig. 17 Parameterized smoothing correction for medium and high frequency errors

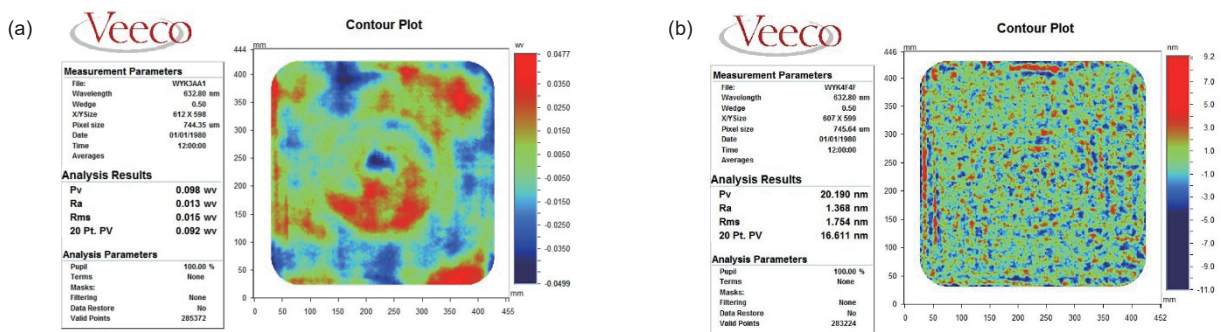


图 18 400 mm \times 400 mm 离轴楔形非球面透镜小工具数控抛光结果。(a) 透过波前误差结果; (b) 中频误差结果

Fig. 18 Results of 400 mm \times 400 mm off-axis wedge aspheric lens by CCOS.

(a) Result of wavefront error; (b) Result of mid-spatial frequency error

4.4 非球面磁流变加工技术

磁流变抛光技术 (Magnetorheological finishing, MRF) 是利用磁流变液在高强度梯度磁场约束作用下的流变性对元件进行抛光, 其独特的剪切加工特性使其在加工过程中不产生机械破碎型缺陷^[43-46], 同时该技术既具有固着磨粒加工高效的优点, 又保留了散粒磨料抛光光滑的优势, 加工确定性高、收敛效率稳定, 在非球面加工领域有着广泛的应用前景^[47]。为了进一步提升非球面加工效果, 本研究团队主要开展了以下工作:

1) 非球面去除函数的理论模型。由于非球面曲率的连续变化, 导致磁流变抛光斑在不同接触区域的形

貌发生改变, 严重影响了磁流变确定性的加工^[48-49]。团队基于流体 Reynolds 方程及磁场理论建立了磁流变去除函数模型, 理论与实际的误差小于 6%(如图 19 所示)。建立了不同曲率下的抛光斑接触模型, 获得了与曲率相关的 MRF 抛光工具的去除效率分布(如图 20 所示)。结合非球面区域化建模方法, 实现了大口径非球面元件的动态去除函数加工能力。

2) 非球面动态驻留时间求解。基于非球面元件不同曲率动态磁流变去除函数, 在非球面驻留时间求解中, 采用了脉冲迭代法的求解思想将去除函数理想化为脉冲函数, 计算整个非球面元件加工的驻留时间, 建立动态驻留时间矩阵, 为非球面元件工艺算法提供

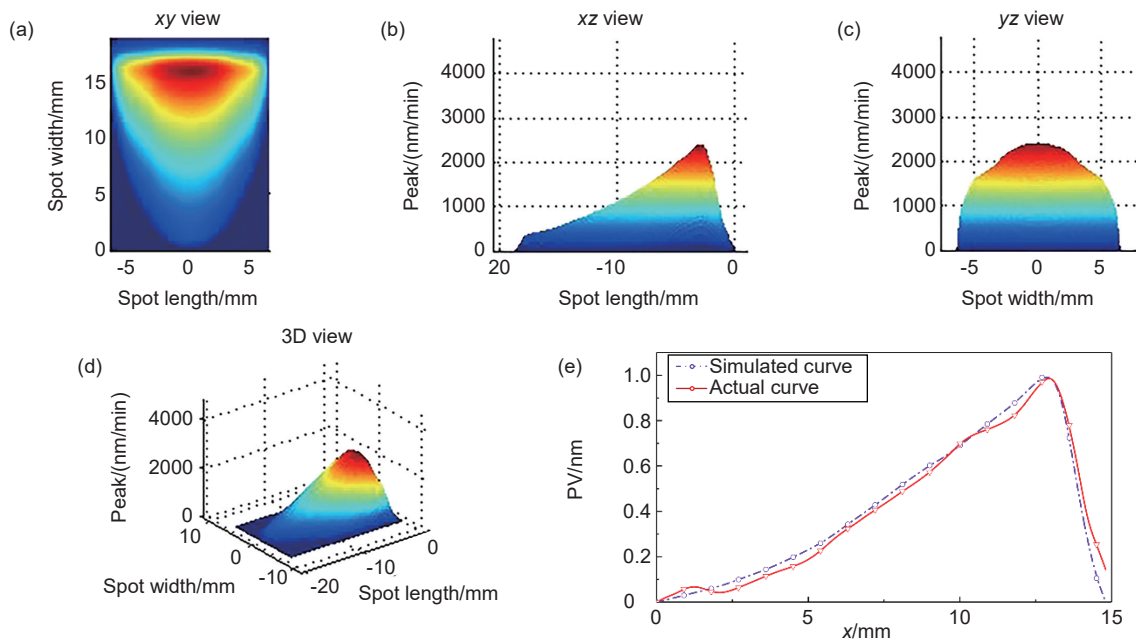


图 19 理论 MRF 去除函数。(a)~(d) 理论去除函数形貌图; (e) 理论与实际去除函数归一化曲线对比

Fig. 19 Theoretical MRF polishing spot. (a)~(d) Theoretical removal function topography; (e) Comparison of theoretical and practical removal function normalization curves

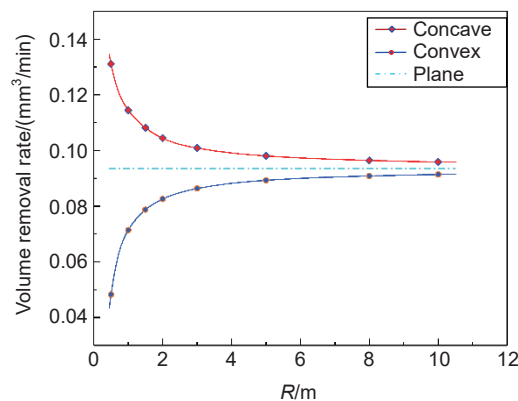


图 20 元件不同曲率与 MRF 抛光斑体积去除率分布曲线

Fig. 20 Optics curvature and MRF polishing spot volume removal rate distribution curve

技术支撑,提高加工确定性。

在 04 专项的支持下,本研究团队联合中物院机械制造工艺研究所开展了磁流变机床国产化研制工作(如图 21 所示),解决了近高斯分布强漏磁场的稳定控制、高粘度大比重抛光液有效匀化与精密传送等关键技术问题,联合工艺研究成果,对 400 mm×400 mm 非球面熔石英元件获得了波前 $PV \leq 0.1\lambda$ 、梯度 $GRMS \leq 2.5 \text{ nm/cm}$ 、粗糙度 $\leq 0.2 \text{ nm}$ 的加工结果。

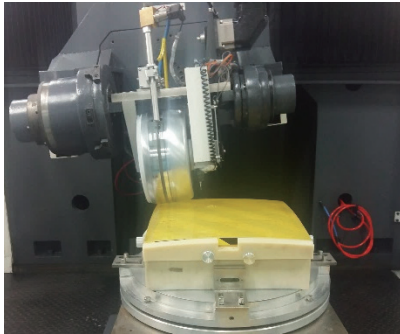


图 21 磁流变加工非球面实物图

Fig. 21 MRF processing aspheric surface

5 结论

本文围绕“超精密、确定性”强激光光学元件全流程制造方法,综述了中物院激光聚变研究中心近几年在大口径强激光光学元件超精密制造技术研究方面开展的相关工作。上述关键技术应用于制造流程线中,实现了批量制造,这些成果为高功率固体激光装置建设以及 ICF 领域的发展奠定了坚实基础。

未来,随着强激光系统综合性能不断提升,迫切需要高性能、高精度以及高质量的光学元器件,对强激光光学元件超精密加工典型需求主要呈现为:1) 光学超精密加工技术朝极端化方向发展,如复杂曲面、纳米级形状精度、亚纳米级超光滑表面等;2) 光学元件表面无损化加工需求迫切,需突破传统研抛加工机理与技术,发展非接触能场加工等新原理、新方法与新技术,实现近无缺陷制造;3) 光学元件批量制造效能亟待提高,进一步提高装备可靠性与稳定性,提升制造柔性化、智能化水平,以建立支撑现代光学系统研制的快速响应能力。

参考文献

[1] Campbell J H, Hawley-Fedder R A, Stolz C J, *et al.* NIF optical materials and fabrication technologies: An overview[J]. *Proceedings of SPIE*, 2004, **5341**: 84–101.

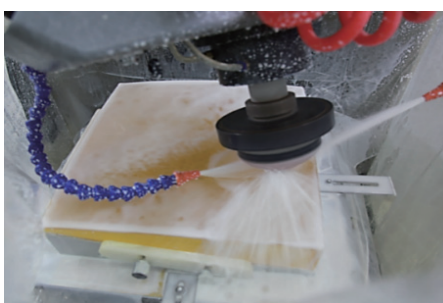
- [2] Xu Q, Wang J, Ma P, *et al.* Progress of advanced optical manufacturing technology[J]. *High Power Laser and Particle Beams*, 2013, **25**(12): 3098–3105.
许乔, 王健, 马平, 等. 先进光学制造技术进展[J]. *强激光与粒子束*, 2013, **25**(12): 3098–3105.
- [3] Spaeth M L, Manes K R, Kalantar D H, *et al.* Description of the NIF laser[J]. *Fusion Science and Technology*, 2016, **69**(1): 25–145.
- [4] Fuchs B A, Hed P P, Baker P C. Fine diamond turning of KDP crystals[J]. *Applied Optics*, 1986, **25**(11): 1733–1735.
- [5] Liang Y C, Chen W Q, Bai Q S, *et al.* Design and dynamic optimization of an ultraprecision diamond flycutting machine tool for large KDP crystal machining[J]. *The International Journal of Advanced Manufacturing Technology*, 2013, **69**(1–4): 237–244.
- [6] Chen M J, Li M Q, Cheng J, *et al.* Study on characteristic parameters influencing laser-induced damage threshold of KH_2PO_4 crystal surface machined by single point diamond turning[J]. *Journal of Applied Physics*, 2011, **110**(11): 113103.
- [7] An C H, Deng C Y, Miao J G, *et al.* Investigation on the generation of the waviness errors along feed-direction on flycutting surfaces[J]. *The International Journal of Advanced Manufacturing Technology*, 2018, **96**(1): 1457–1465.
- [8] Yang X, An C H, Wang Z Z, *et al.* Research on surface topography in ultra-precision flycutting based on the dynamic performance of machine tool spindle[J]. *The International Journal of Advanced Manufacturing Technology*, 2016, **87**(5–8): 1957–1965.
- [9] Zhang F H, Wang S F, An C H, *et al.* Full-band error control and crack-free surface fabrication techniques for ultra-precision fly cutting of large-aperture KDP crystals[J]. *Frontiers of Mechanical Engineering*, 2017, **12**(2): 193–202.
- [10] Wang S F, An C H, Zhang F H, *et al.* An experimental and theoretical investigation on the brittle ductile transition and cutting force anisotropy in cutting KDP crystal[J]. *International Journal of Machine Tools and Manufacture*, 2016, **106**: 98–108.
- [11] Wang S F, An C H, Zhang F H, *et al.* Simulation research on the anisotropic cutting mechanism of KDP crystal using a new constitutive model[J]. *Machining Science and Technology: An International Journal*, 2017, **21**(2): 202–222.
- [12] Guo Y B, Chen B K, Zhang Y, *et al.* Research on parallel grinding method of non-axisymmetric aspheric lens[J]. *Chinese Journal of Mechanical Engineering*, 2004, **17**(1): 149–151.
- [13] Shore P, Morantz P, Luo X C, *et al.* Big OptiX ultra precision grinding/measuring system[J]. *Proceedings of SPIE*, 2005, **5965**: 241–248.
- [14] Suzuki H, Murakami S. An ultraprecision grinding machine for non-axisymmetric aspheric mirrors[J]. *Nanotechnology*, 1995, **6**(4): 152–157.
- [15] Zhou L, Wei Q C, Zhao S J, *et al.* Computer-aided NC programming system for large scale and off-axis aspheric optics in parallel grinding[J]. *Proceedings of SPIE*, 2019, **10842**: 108420V.
- [16] Zhou L, Wei Q C, Zheng N, *et al.* Dressing technology of arc diamond wheel by roll abrading in aspheric parallel grinding[J]. *The International Journal of Advanced Manufacturing Technology*, 2019, **105**(5): 2699–2706.
- [17] Zhou L, Xie R Q, Chen X H, *et al.* Analysis and optimization on cross section profile of fused silica grinding wheel[J]. *Diamond and Abrasives Engineering*, 2018, **38**(1): 59–64.
周炼, 谢瑞清, 陈贤华, 等. 熔石英磨削砂轮截面轮廓分析与优化[J]. *金刚石与磨料磨具工程*, 2018, **38**(1): 59–64.

- [18] Zhou L, Zheng N, Chen X H, *et al.* Crack depth uniformity control techniques for large scale fused silica optics in grinding process[J]. *Proceedings of SPIE*, 2019, **11068**: 1106815.
- [19] Zhou L, Wei Q C, Li J, *et al.* The effect of diamond wheel wear on surface and sub-surface quality in fused silica optics grinding[J]. *IOP Conference Series Materials Science and Engineering*, 2019, **677**: 022091.
- [20] Walker D D, Brooks D, Freeman R, *et al.* The first aspheric form and texture results from a production machine embodying the precession process[J]. *Proceedings of SPIE*, 2001, **4451**: 267–276.
- [21] Pan R, Zhong B, Chen D J, *et al.* Modification of tool influence function of bonnet polishing based on interfacial friction coefficient[J]. *International Journal of Machine Tools and Manufacture*, 2018, **124**: 43–52.
- [22] Zhong B, Wang C J, Chen X H, *et al.* Time-varying tool influence function model of bonnet polishing for aspheric surfaces[J]. *Applied Optics*, 2019, **58**(4): 1101–1109.
- [23] Zhong B, Chen X H, Deng W H, *et al.* Improving material removal determinacy based on the compensation of tool influence function[J]. *Proceedings of SPIE*, 2018, **10710**: 107102P.
- [24] Zhong B, Huang H Z, Chen X H, *et al.* Modelling and simulation of Mid-spatial-frequency error generation in CCOS[J]. *Journal of the European Optical Society-Rapid Publications*, 2018, **14**(1): 4.
- [25] Zhong B, Chen X H, Pan R, *et al.* The effect of tool wear on the removal characteristics in high-efficiency bonnet polishing[J]. *The International Journal of Advanced Manufacturing Technology*, 2017, **91**(9): 3653–3662.
- [26] Zhong B, Huang H Z, Chen X H, *et al.* Impact of pad conditioning on the bonnet polishing process[J]. *The International Journal of Advanced Manufacturing Technology*, 2018, **98**(1): 539–549.
- [27] Chen X H, Yu H D, Zhong B, *et al.* Development of key technologies in the fabrication of large aperture off-axis wedge focusing lens[J]. *Proceedings of SPIE*, 2016, **10255**: 102551C.
- [28] Ke X L, Wang C J, Guo Y B, *et al.* Modeling of tool influence function for high-efficiency polishing[J]. *The International Journal of Advanced Manufacturing Technology*, 2016, **84**(9–12): 2479–2489.
- [29] Pal R K, Garg H, Karar V. Full aperture optical polishing process: overview and challenges[C]//*CAD/CAM, Robotics and Factories of the Future*, New Delhi, 2016: 461–470.
- [30] Surawala T I, Feit M D, Steele W A. Toward Deterministic Material removal and surface figure during fused silica pad polishing[J]. *Journal of the American Ceramic Society*, 2010, **93**(5): 1326–1340.
- [31] Xie R Q, Zhao S J, Liao D F, *et al.* Recent advances in rapid polishing process of large aperture optical flats[J]. *Proceedings of SPIE*, 2019, **10841**: 108410V.
- [32] Xie R Q, Zhao S J, Liao D F, *et al.* Suppressing surface low and mid-spatial frequency errors of large optics during full-aperture rapid polishing[C]//*Optical Fabrication and Testing 2019*, OSA Technical Digest, Washington, DC United States, 2019: OM3A.2.
- [33] Xie R Q, Zhao S J, Liao D F, *et al.* Numerical simulation and experimental study of surface waviness during full aperture rapid planar polishing[J]. *The International Journal of Advanced Manufacturing Technology*, 2018, **97**(9): 3273–3282.
- [34] Xie R Q, Zhao S J, Liao D F, *et al.* Effects of kinematics and groove parameters on the mid-spatial frequency error of optics induced during full aperture polishing[J]. *Precision Engineering*, 2019, **57**: 176–188.
- [35] Xie R Q, Liao D F, Chen J, *et al.* In-situ shape measurement technology during large aperture optical planar continuous polishing process[J]. *Proceedings of SPIE*, 2018, **10710**: 1071033.
- [36] Liao D F, Xie R Q, Sun R K, *et al.* Improvement of the surface shape error of the pitch lap to a deterministic continuous polishing process[J]. *Journal of Manufacturing Processes*, 2018, **36**: 565–570.
- [37] Liao D F, Xie R Q, Zhao S J, *et al.* Surface shape development of the pitch lap under the loading of the conditioner in continuous polishing process[J]. *Journal of the American Ceramic Society*, 2019, **102**(6): 3129–3140.
- [38] Liao D F, Zhang F H, Xie R Q, *et al.* Deterministic control of material removal distribution to converge surface figure in full-aperture polishing[J]. *Journal of Manufacturing Processes*, 2020, **53**: 144–152.
- [39] Liao D F, Zhang F H, Xie R Q, *et al.* Effect of interfacial friction force on material removal in full aperture continuous polishing process[J]. *Precision Engineering*, 2020, **63**: 214–219.
- [40] Kim D W, Park W H, An H K, *et al.* Parametric smoothing model for visco-elastic polishing tools[J]. *Optics Express*, 2010, **18**(21): 22515–22526.
- [41] Kim D W, Burge J H. Rigid conformal polishing tool using non-linear visco-elastic effect[J]. *Optics Express*, 2010, **18**(3): 2242–2257.
- [42] Song C, Walker D D, Yu G Y. Misfit of rigid tools and interferometer subapertures on off-axis aspheric mirror segments[J]. *Optical Engineering*, 2011, **50**(7): 073401.
- [43] Peng W Q, Li S Y, Guan C L, *et al.* Ultra-precision optical surface fabricated by hydrodynamic effect polishing combined with magnetorheological finishing[J]. *Optik*, 2018, **156**: 374–383.
- [44] Hou J, Wang H X, Chen X H, *et al.* Effect of magnetorheological processing parameters on polishing spots[J]. *Proceedings of SPIE*, 2018, **10847**: 108470P.
- [45] Patel R. Mechanism of chain formation in nanofluid based MR fluids[J]. *Journal of Magnetism and Magnetic Materials*, 2011, **323**(10): 1360–1363.
- [46] Susan-Resiga D, Bica D, Vékás L. Flow behaviour of extremely bidisperse magnetizable fluids[J]. *Journal of Magnetism and Magnetic Materials*, 2010, **322**(20): 3166–3172.
- [47] Menapace J A, Ehrmann P E, Bayramian A J, *et al.* Imprinting high-gradient topographical structures onto optical surfaces using magnetorheological finishing: manufacturing corrective optical elements for high-power laser applications[J]. *Applied Optics*, 2016, **55**(19): 5240–5248.
- [48] Hou J, Cao M C, Wang H X, *et al.* Determination of optimized removal functions for imprinting continuous phase plates using fuzzy theory[J]. *Applied Optics*, 2018, **57**(21): 6089–6096.
- [49] Hou J, Liao D F, Wang H X. Development of multi-pitch tool path in computer-controlled optical surfacing processes[J]. *Journal of the European Optical Society-Rapid Publications*, 2017, **13**(1): 22.

Progress on ultra precision manufacturing technology of large-aperture high-power laser optics

Fan Fei, Xu Xi, Xu Qiao*, Wang Jian, Zhong Bo, Xie Ruiqing, Lei Xiangyang,
Chen Xianhua, Wang Shengfei, Hou Jing, Deng Wenhui, An Chenhui,
Zhou Lian, Zhao Shijie, Liao Defeng, Zhu Yujie

Research Centre of Laser Fusion, China Academy of Engineering Physics, Mianyang, Sichuan 621900, China



Bonnet polishing picture

Overview: The high-power solid-state laser facility for inertial confinement fusion is the largest optical system with the most complex structure. It requires tens of thousands of large-aperture high-power laser optics, including phosphate neodymium glass amplifier, plane mirrors, aspheric focusing lens, diffraction elements, and nonlinear laser crystals. In order to further improve the beam quality and realize the stable operation under high laser flux, these large-aperture optics are required to precisely control the full-spatial frequency error, and realize efficient mass-manufacturing. This review summarizes the recent critical progress in the field of ultra-precise manufacturing of large-aperture optics for high-power laser facility, especially for the technology and equipment of single point diamond fly-cutting, aspheric ultra-precision grinding, and deterministic polishing. In addition, the application status of these key technologies in the mass-manufacturing flow-line is stated specifically. Moreover, with the continuous improvement of comprehensive performance for high-power laser facility, the typical requirements for ultra-precise manufacturing of high-power laser optics are as follows: 1) The development of advanced optical manufacturing technology will march towards the extreme conditions, such as complex aspheric structures, nano-scale shape control, sub-nanometer ultra-smooth surface, etc. 2) The damage-free machining over optical surfaces is in urgent demand, and it is necessary to break through the traditional polishing mechanism and technology, in order to develop novel principles, methods and technologies to realize near non-defect manufacturing. 3) The efficiency of mass manufacturing of optics needs to be improved, and further improvement of the reliability and stability of equipment, as well as the enhancement of flexible and intelligent manufacturing is of great demand. This will help to establish the fast response ability to support the research and development on modern optical system.

Citation: Fan F, Xu X, Xu Q, *et al.* Progress on ultra precision manufacturing technology of large-aperture high-power laser optics[J]. *Opto-Electronic Engineering*, 2020, 47(8): 200135

Supported by National Science and Technology Major Project of the Ministry of Science and Technology of China (2017ZX04022001-101)

* E-mail: xuqiao@vip.sina.com